

H α emission line profiles of selected post-AGB stars

Griet C. Van de Steene & Peter R. Wood

*RSAA (ANU), Mount Stromlo Observatory, Private Bag, Weston
Creek, ACT 2611, Australia*

Peter A.M. van Hoof

*CITA, McLennan Labs, 60 St. George Street, Toronto, ON M5S 3H8,
Canada*

Abstract.

We present H α emission line spectra of 7 post-AGB stars. Typically, they have a P-Cygni type profile with a very strong emission component and a relatively narrow absorption component. These lines are formed in the fast post-AGB wind which in most cases has a velocity of around 100 km/s. Hence the emission originates close to the central star and the absorption occurs in the fast wind itself or in the region where the fast wind sweeps up the slow wind. The emission profile has very broad wings. It is still unclear what causes these wings.

1. Introduction

A most intriguing challenge is to understand how Asymptotic Giant Branch (AGB) stars transform their surrounding mass-loss shells in a couple of thousand years into the variety of shapes and sizes observed in Planetary Nebulae (PNe). There are a number of theories currently being investigated. In the generalized interacting stellar wind model, a variety of axisymmetric PN shapes are obtained by the interaction of a very fast central star wind with the progenitor AGB circumstellar envelope (Kwok 1982), when the latter is denser near the equator than the poles (Frank et al. 1993). Sahai & Trauger (1998) proposed that the primary agent for shaping PNe is not the density contrast, but a high speed collimated outflow of a few 100 km/s. No consensus about the dominant physical process responsible for the shaping of PNe has emerged so far, but there is agreement that they occur during the early AGB-to-PN transition stage. However, the details of the rates of evolution and the strength of the stellar winds during the AGB-to-PN transition phase are very poorly known, either theoretically or observationally. To remedy this we have started to study a sample of post-AGB objects spectroscopically.

2. Observations

Objects with far infrared colors typical of PNe were selected from the IRAS catalogue. Apart from PNe, only post-AGB stars are typically found in this part

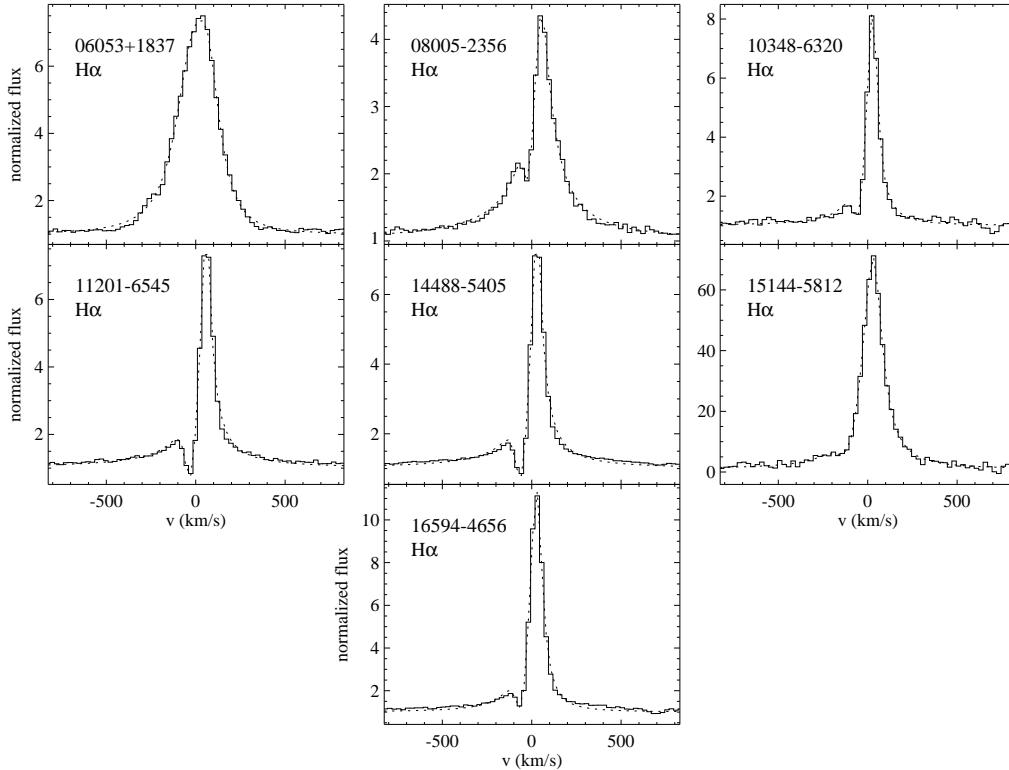


Figure 1. Plots of the H α profiles of the post-AGB stars (solid lines) with the fits over-plotted (dotted lines).

of the color-color diagram. Furthermore, the objects selected were not detected in the radio continuum above a detection limit of 3 mJy (Van de Steene & Pottasch 1993). Hence they don't seem to have evolved to the PN stage as yet.

We obtained JHKL images of the candidates with CASPIR on the 2.3-m telescope at Siding Spring Observatory in Australia in order to obtain accurate positions for the IRAS counterparts. Subsequently, high resolution optical spectra were obtained with the Double Beam Spectrograph on the 2.3-m telescope. The resolution was 0.55 \AA per pixel.

We present H α profiles of selected post-AGB stars showing H α in emission. Obviously not all objects showed H α in emission, some have H α in absorption and some show neither H α emission or absorption. Some of the post-AGB stars detected in the near infrared could not be seen in the optical due to large extinction.

3. H α emission line profiles

The wings are not fitted well when only gaussian profiles are used. We fitted the H α emission lines with the sum of a 'generalized' Lorentz emission profile and a gaussian absorption profile. A 'generalized' Lorentz profile is defined as $F_\lambda \propto 1/[1 + (\Delta\lambda/\lambda_w)^\alpha]$ with λ_w (the HWHM of the profile) and α as free

parameters. For $\alpha = 2$ this is the familiar Lorentz profile. Since all observed profiles are wider on the blue side, the HWHM of the fitted profile was allowed to have different values in the red and the blue part (across the absorption). The results of the fits are shown in Table 1. The listed absolute flux is for the whole, integrated profile and has not been dereddened. The listed FWHM is the sum of the blue and red HWHM. The entries v_{abs} and v_{emm} are the velocities of the center of the absorption and the emission peak relative to the systemic velocity. We determined the systemic velocity from photospheric absorption lines using C II at 6578.05 Å and 6582.88 Å and He I at 6678.15 Å, if detected. We used the equivalent widths of these lines to determine the spectral types of the objects by comparing them with the results of Lennon et al. (1993). We calculated the terminal velocity of the wind v_{∞} from the blue edge of the absorption in the H α profile according to: $v_{\infty} = \text{FWHM}_{\text{abs}} - v_{\text{abs}}$.

Table 1. Fit parameters for the H α emission lines.

Object IRAS	Spec. Type	Flux 10^{-16} W/m ²	FWHM km/s	α	v_{abs} km/s	v_{emm} km/s	v_{∞} km/s
06053+1837		3.13	253	2.63	—	—	—
08005–2356		8.38	149	1.45	–16	57	72
10348–6320	B4	0.78	77	1.78	–48	30	114
11201–6545	A0	5.63	75	1.45	–24	61	99
14488–5405	B9Ia	19.15	79	1.49	–55	31	131
15144–5812		0.41	135	1.98	—	—	—
16594–4656	B7	2.55	93	1.99	–49	28	126

4. Interpretation

The similarity in the H α profiles leads us to suggest the following interpretation of our observations.

Trammel et al. (1994) determined that the H α emission of IRAS 08005–2356 was polarized. Based on the polarization angles, they suggested a bipolar geometry for this object. A bipolar geometry was also suggested for IRAS 16594–4656 based on HST images by Hrivnak et al. (1999). Based on the similarity of the presented emission line profiles, quite a few of our objects could be bipolar PNe.

The lack of other forbidden emission lines in the spectra indicates that the H α emission is not due to photo-ionization of the shell. IRAS 16594–4656 is the only star in our sample for which [O I] emission was observed. No [N II] or [S II] emission was detected in any of the spectra. Consequently the main H α emission cannot be caused by shock emission either. The blue peak in the H α emission is too faint compared to the red peak to originate from a disk or expanding shell.

The P-Cygni type of the H α profiles indicates the presence of a strong stellar wind which can produce the emission line and the blue-shifted absorption. The terminal velocity of the wind can be derived from the position of the blue absorption edge. The velocity of the fast wind is around 100 km/s. No value for v_{∞} could be determined for IRAS 06053+1837 and IRAS 15144–5812, but indications are that they have a higher velocity than the rest of the sample.

The absorption is too deep to be photospheric, hence the absorption must be produced outside the emission region. For post-AGB stars the fast stellar wind is encircled by the slower AGB wind, which can absorb line photons produced by the fast wind. The velocity of the center of the absorption is similar to the AGB wind velocity or higher. This suggests that the absorption occurs in the fast wind itself or in the region where the fast wind sweeps up the slow wind.

The $H\alpha$ profiles show very extended wings, which we can follow in our spectra up to ~ 500 km/s and even 1500 km/s for IRAS 08005–2356. In the case of HD101584, a type B9II post-AGB star with a spectrum very similar to our sample, Bakker et al. (1996) attributed the wings to electron scattering by free electrons in the stellar wind. However, Thomson scattering is wavelength independent and the fact that we don't see wings in our $Br\gamma$ spectra argues against this. Multiple Rayleigh scattering off neutral hydrogen in the expanding AGB shell or multiple scattering off dust grains in that same shell may be able to produce these wings as well. However, Rayleigh scattering has too low a cross section to be of much importance in a dusty environment like a post-AGB star. Grain scattering is supported by Trammell et al. (1994) who suggested that the polarization of $H\alpha$ was most likely caused by scattering off dust grains in a dense torus surrounding the central star in IRAS 08005–2356. However, for both cases, the fact that the observed velocities in the wings are so much larger than the AGB or post-AGB wind velocities casts doubt on this explanation. To reach the observed velocities the scattering must occur in the wind or maybe in a Keplerian disk, if there is one. It is still unclear what causes them.

Extended wings have also been observed in young compact PNe such as M2–9 (Balick 1989), Mz–3 (López & Meaburn 1983), Cn 3–1 and M3–27 (Miranda et al. 1997). No profound explanation for these wings has been proposed in the literature.

References

- Bakker, E.J., Lamers, H.J.G.L.M., Waters, L.B.F.M., Waelkens, C., Trams, N.R., and Van Winckel, H. 1996, *A&A*, 307, 869
- Balick, B. 1989, *AJ*, 97, 476
- Frank, A., Balick, B., Icke, V., and Mellema, G. 1993, *ApJ*, 404, L25
- Hrivnak, B.J., Kwok, S., and Su, K.Y.L. 1999, *ApJ*, in press
- Kwok, S. 1982, *ApJ*, 258, 280
- Lennon, D.J., Dufton, P.L., and Fitzsimmons A. 1993, *A&AS*, 97, 559
- López, J.A., and Meaburn, J., 1983 *MNRAS*, 204, 203
- López, J.A., Steffen, W., and Meaburn, J. 1997, *ApJ*, 485, 697
- Miranda, L.F., Vázquez, R., Torrelles, J.M., Eiroa, C., and López, J.A. 1997, *MNRAS*, 288, 777
- Sahai, R., and Trauger, J.T. 1998, *AJ*, 116, 1357
- Trammell, S.R., Dinerstein, H.L., and Goodrich, R.W. 1994, *AJ*, 108, 984
- Van de Steene, G.C., and Pottasch, S.R. 1993, *A&A*, 274, 895